Electronic Supplementary Information for:

Tunable Synthesis of Magnetoelectric $CoFe_2O_4$- $BaTiO_3$ Core-Shell Nanowires

Noah D. Ferson[a], John R. Ganiban[a], David P. Arnold[b], and Jennifer S. Andrew[a]

[a]Dept. of Materials Science & Engineering, University of Florida, Gainesville, FL 32611, USA.

[b]Dept. of Electrical & Computer Engineering, University of Florida, Gainesville, FL 32611, USA.

* Corresponding authors: jandrew@mse.ufl.edu

Core-Shell Nanowire Synthesis

$BaTiO_3$ Shell Fabrication:

In the first step of the core-shell nanowire synthesis, a $BaTiO_3$ shell is deposited along the pore walls of the anodic aluminum oxide (AAO) template. Templates for this work were purchased from two suppliers: Whatmann PLC and Top Membranes Technology, both having a nominal pore diameter of 200 nm and thickness of 60 μm. Before use, templates were degreased via ultrasonic cleaning in acetone, rinsed with deionized water, and then dried under vacuum. A 0.32 M $BaTiO_3$ sol-gel solution was prepared by dissolving barium acetate in glacial acetic acid, followed by the addition of absolute ethanol and titanium isopropoxide such that the Ba^{2+}:Ti^{4+} ratio is 1:1. The sol-gel solution was then allowed to age at room temperature for 30 minutes before use. To wet the AAO template with the $BaTiO_3$ sol-gel, 250 uL of the solution is drop-cast onto the template surface and then placed into a 3D-printed polypropylene vacuum chamber. Vacuum is pulled for three minutes and then the sample is spin coated at 500 rpm for 10s and then quickly ramped to 2000 rpm for 40s. Next, the samples were dried on a hot plate set to 150 °C for 5 minutes. This template wetting procedure was repeated up to five times in this work to increase the thickness of the $BaTiO_3$ shell. To crystallize the amorphous $BaTiO_3$ shell, the sample was calcined in air at 650 °C for 6 hours. It was found that placing the template with $BaTiO_3$ shells between two ceramic dishes, prevented curling that could be detrimental to subsequent processing steps. The $BaTiO_3$ yield was determined by weighing the empty template (W_o) before sol-gel template wetting and after the wetting process and calcination (W_i) according to eqn. S1:

$$BaTiO_3 Yield\ (wt\%) = \frac{W_i - W_o}{W_o} * 100 \qquad \text{(S1)}$$

$CoFe_2O_4$ Core Deposition:

The surface of the AAO template with $BaTiO_3$ shells is coated with 400 nm of Cu via sputter deposition to serve as the working electrode during electrodeposition. It was observed during the fabrication of $CoFe_2O_4$ nanowires that the sputtered Cu layer was highly porous. To fill the voids left after sputter deposition, a subsequent Cu electroplating step was necessary. This step was found to be key in order to obtain free standing core-shell nanowires from the AAO template after the preferential etching of Cu and AAO. Otherwise, $CoFe_2$ will deposit within the porous Cu

film and result in bundled nanowire films. Cu electroplating was performed for 10 minutes in a bath of 1.56 M copper sulfate and 0.47 M H_2SO_4 (aq) using a copper foil cathode at a current density of 5 mA/cm^2.

Three-electrode electrodeposition was performed with a Princeton Applied Research Potentiostat (Model 263A), where the Cu coated AAO template with $BaTiO_3$ shells sample served as the working electrode, a platinized stainless-steel mesh as the counter electrode, and an $Ag/AgSO_4$ reference electrode. The electrodeposition bath consisted of 0.02 M cobalt sulfate, 0.03 M ferrous sulfate, 0.23 M ammonium sulfate, and 0.125 M boric acid and was pH adjusted to 3.0 with 0.5 M sulfuric acid. During electrodeposition, the solution was continuously stirred, and a NdFeB magnet was placed behind the working electrode. Electrodeposition durations were varied from 30 minutes up to 2 hours at -1.2 V vs $Ag/AgSO_4$. Longer deposition durations were used to obtain longer nanowires. After electrodeposition, the Cu back electrical contact was etched using Blue Etch (saturated copper sulfate in 30% ammonium hydroxide) and then rinsed 3 times in deionized water. The $CoFe_2$ alloy was then oxidized through a heat treatment at 600 °C for 24 hours. To release the core-shell nanowires from the template, AAO is preferentially etched in 2M NaOH. The nanowires are then rinsed five times in deionized water and dried under vacuum to obtain a core-shell nanowire powder.

Material Characterization

The morphology of core-shell nanowires was investigated using scanning electron microscopy (SEM; Tescan MIRA3), focused ion beam SEM (FIB-SEM; FEI Helios G4 PFIB CXe DualBeam) and scanning transmission electron microscopy (STEM; FEI Talos F200I). Phase identification was conducted using X-ray diffraction (XRD) (Panalytical XPert Powder) with a Cu K_α source ($\lambda_{K_{\alpha 1}}$=1.54059 Å) over the range of 20 - 80 °2θ. Fig. S1 shows representative diffraction patterns of the nanowires after they were released from their templates via wet chemical etching using 2M NaOH. The XRD patterns exhibit a poor signal to noise ratio, partly due to the nanocrystalline structure of the nanowires, which causes peak broadening in the diffraction patterns, thus making the data a poor candidate for Reitveld refinement. Therefore, the peaks present in the diffraction patterns were indexed for phase identification. Characteristic peaks at 31.5, 38.8, 45.1, and 56.1 °2θ confirm the formation of perovskite $BaTiO_3$, which correspond to the (101), (111), (200), and (211) family of planes, respectively. Characteristic peak splitting at

ca. 45 $^{o}2\theta$ (44.82 and 45.41 $^{o}2\theta$), corresponding the (200) and (002) reflections, is often used to identify the tetragonal phase of $BaTiO_3$. However, the nanocrystalline nature of the $BaTiO_3$ nanotubes made it difficult to resolve this level of detail in the presented XRD patterns.[1] Cubic spinel $CoFe_2O_4$ was identified with observation of peaks present at 30.2, 35.6, 53.6 57.1, and 62.7 $^{o}2\theta$ corresponding to the (220), (311), (422), (333) and (440) family of planes, respectively. Crystallite sizes for $CoFe_2O_4$ were determined from the diffraction patterns presented in Fig. S1 using Scherrer's analysis according to eqn. S2.

$$\tau = \frac{k\lambda}{\beta cos\theta} \qquad \text{(S2)}$$

Where τ is the crystallite size, k is a shape factor (assumed to be 0.9 for spherical crystallites), λ is the X-ray wavelength, β is the full width at half maximum value, in radians, and θ is the Bragg angle, also in radians. Average crystallite sizes were determined to be 16.5 nm for $CoFe_2O_4$, 17.6 nm for 1x wet $CoFe_2O_4$-$BaTiO_3$, and 14.1 nm for 3x wet $CoFe_2O_4$-$BaTiO_3$ nanowires.

For the intended application of the nanocomposites to be used as magnetoelectric transducers, the tetragonal phase is necessary to provide a non-centrosymmetric lattice for piezoelectric behavior in the $BaTiO_3$ shell. Therefore, Raman spectroscopy was used to investigate the local structure of the $BaTiO_3$ nanotubes for phase identification using a Renishaw inVia spectrometer. Spectra were collected after excitation with a 633 nm HeNe laser at 5 mW power in the backscattering geometry over the range of 100–1000 cm^{-1}. The incident laser was polarized in the x-direction. Further polarization states were not investigated within this work. In preparation for Raman spectroscopy, free-standing nanotubes were drop-cast onto silicon substrates. The room temperature Raman spectra presented in Fig. S2 closely agrees with those reported for nanocrystalline tetragonal $BaTiO_3$ in the literature.[1–3] The peaks present at 185 and 715 cm^{-1} have been assigned to the transverse optical (TO) and longitudinal optical (LO) phonon modes with A_1 symmetry, respectively.[2] While the distinct peak at 307 cm^{-1} has been assigned to the B_1 + E(TO + LO) phonon modes and is indicative of asymmetry within the TiO_6 octahedra on the local scale.[2,3] Identifying the band present at ca. 515 cm^{-1} is difficult because the samples were prepared on a Si substrate, which has a prominent peak at ca. 520.5 cm^{-1}. Ultimately, the Raman spectra shown in Fig. S2 indicates presence of tetragonal ordering in the $BaTiO_3$ nanotubes.

Magnetoelectric Coupling Investigation

Magnetoelectric coupling in the core-shell nanowires has been observed using magnetometry after electrically poling the nanowires. Electric polarization was completed using a home-built corona discharge poling station, as depicted in Fig. S3. In short, a high voltage power supply (Glassman High Voltage Inc, PS/EL30R01.5) was connected to a micromachined copper needle and ground stainless steel plate. The ground plate was placed on a hot plate with an attached thermocouple to monitor temperature during the poling process. Nanowire samples were prepared by drop casting a concentrated solution of nanowires in deionized water onto aluminum foil substrates. During solvent evaporation, nanowires were magnetically aligned using two NeFeB permanent disc magnates that produced a field of 65 mT. Then, samples are heated to 70 °C and poled under an applied voltage of 8.5 kV with a needle to ground distance of 15 mm. In this configuration, the applied voltage is perpendicular to the nanowire long axis. A stable corona is applied for 15 minutes, after which the samples were removed from the hot plate and quickly transferred to a stainless-steel plate to cool down to room temperature. The applied voltage and distance values were optimized to obtain a stable corona for the duration of the poling experiments. Estimating an exact electric field across the nanowires during the poling process is challenging because the nanowire films were assembled stochastically, and thus, an average thickness was not determined.

Vibrating sample magnetometry (VSM) using an ADE Tech. EV-9 VSM with max fields of ±1,800 kA/m was used to collect dc magnetic hysteresis loops of core-shell nanowires, both after electric polarization and after thermal depolarization. Thermal depolarization was performed in situ using the furnace equipped on the VSM by heating the nanowires to 180 °C and holding for 15 minutes. We chose 180 °C to ensure that the nanowires were heated well above the Curie temperature of $BaTiO_3$, which is 120 °C. Samples were then cooled to room temperature before collecting the post depolarization hysteresis loops. Hysteresis loops were collected starting from zero applied field and increasing to 1,800 kA/m to initially saturate samples. This initial magnetization segment was excluded from analysis to ensure each sample had reached saturation prior to conducting analysis. However, complete hysteresis loops are shown Fig. S4 for completeness.

Magnetization versus temperature measurements have been performed on core-shell nanowires as an indirect method to probe magnetoelectric coupling using superconducting quantum interference device (SQUID) magnetometry (Quantum Design MPMS3). As the nanowires are cooled from 300K, there is a distinct change in magnetization near the orthorhombic to rhombohedral phase transition of $BaTiO_3$ (170 K) for the sample that has undergone three $BaTiO_3$ wetting cycles as shown in Fig. S5.

Anisotropy Investigations

The effective anisotropy constants (K_{eff}) were determined using an approach adapted from ref [4]. Magnetization measurements were made on nanowires while they were still embedded within their template. As these nanocomposites are intended for room temperature applications, all magnetic hysteresis loops were collected at room temperature. In these measurements, the applied magnetic field was either parallel or perpendicular to the nanowire's long axis, which corresponds to the magnetic easy and hard axes, respectively. It is important to note that K_{eff} was quantified using eqn. (1) (as seen in the main text) where magnetization values were standardized to the saturation magnetization value for measurements taken perpendicular and parallel to the nanowire's long axis. This choice was driven by the fact that we cannot accurately determine the volume of magnetic material deposited within the template. We expect that even though the magnitude of K_{eff} is not suitable for direct comparison with values reported in the literature, the overall trends observed in this study are still valid. That being, the effective anisotropy in the core-shell magnetoelectric nanowires can be modulated by both the nanowire length (or aspect ratio) and the spacing between neighboring wires, by increasing the thickness of the $BaTiO_3$ shell.

The average nanowire diameter distribution is dictated by the pore diameter distribution of the AAO templates used in this work. The distribution of pore diameters will have direct implication of the filling factor (P), or porosity, of the AAO template. P can be defined by eqn. S2.[5]

$$P = \frac{2\pi}{\sqrt{3}}\left(\frac{r}{D_{int}}\right)^2 \qquad \text{(S2)}$$

Where r is the pore radius and D_{int} is the interpore spacing of the template. Using imageJ analysis the pore size distribution was determined and is presented in Fig. S6. From this, values for r and D_{int} were determined to be 99.8 +/- 9.4 nm and 489 +/- 33.4 nm, respectively. With these average values, a filling factor (P) of 0.15476 +/- 0.036 was determined. Assessing values for r, D_{int}, and P is challenging due to systematic errors introduced during the measurement process (e.g., image thresholding and segmentation in ImageJ). These errors make it difficult to report a representative value with absolute accuracy. However, for the sample set characterized in this work, the magnitude of the calculated anisotropy values exceeds what can be attributed to error, thus strongly supporting the key conclusions presented within this work.

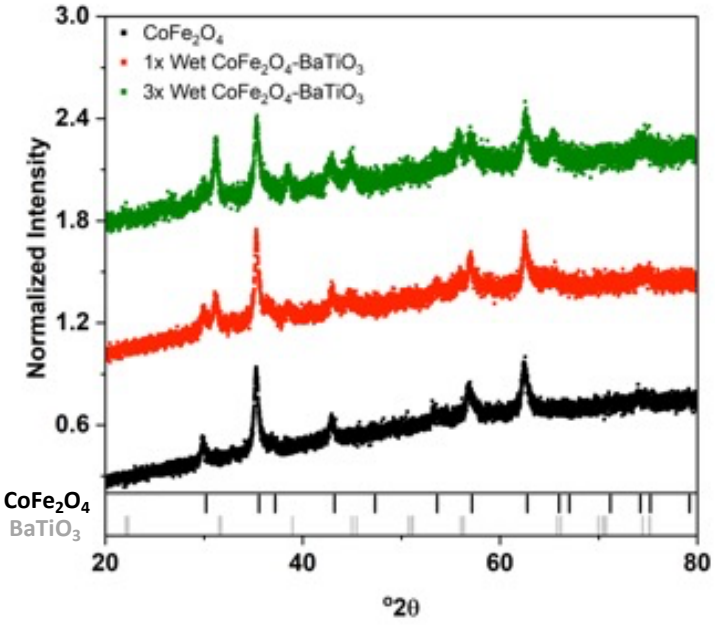

Figure S1. X-ray diffraction patterns for $CoFe_2O_4$ nanowires (black), core-shell nanowires prepared with one (red) $BaTiO_3$ wetting cycle and three (green) $BaTiO_3$ wetting cycles. Rug plot for cubic spinel $CoFe_2O_4$ (ICDD PDF #: 00-066-0244) and tetragonal perovskite $BaTiO_3$ (ICDD PDF#: 01-071-4894) are shown for reference.

Figure S2. Raman spectra for $BaTiO_3$ nanotubes prepared on a silicon substrate. Peaks present at c.a. 185, 307, and 715 cm^{-1} are attributed to the tetragonal phase for $BaTiO_3$.

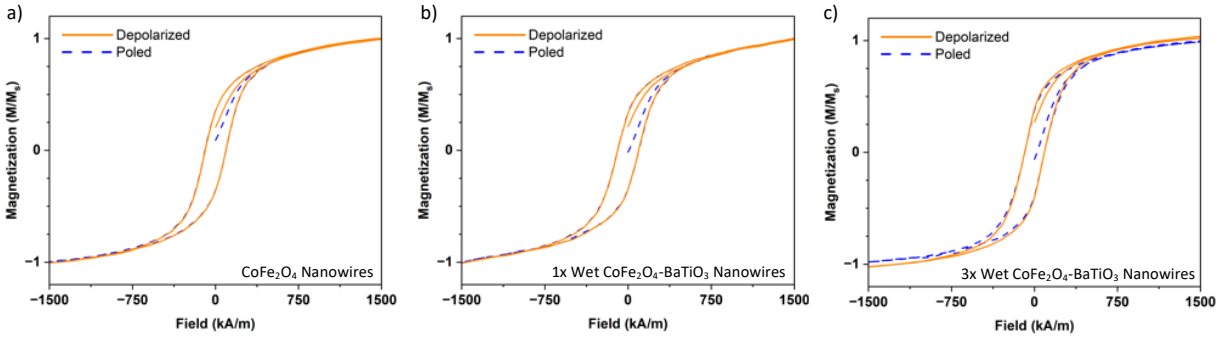

Figure S3. Magnetization vs field data for ex situ poled nanowires via a corona discharge

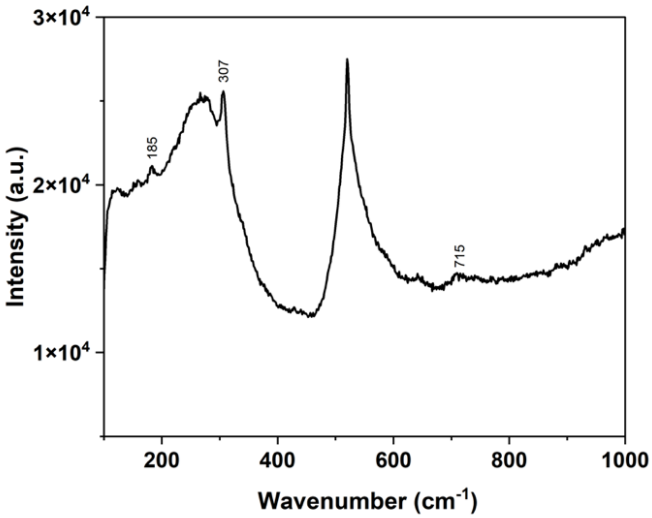

process (blue) and post in situ thermal depolarization (orange) for (a) CoFe2O4 nanowires, core-shell nanowires prepared with one (b) $BaTiO_3$ wetting cycle and three (c) $BaTiO_3$ wetting cycles.

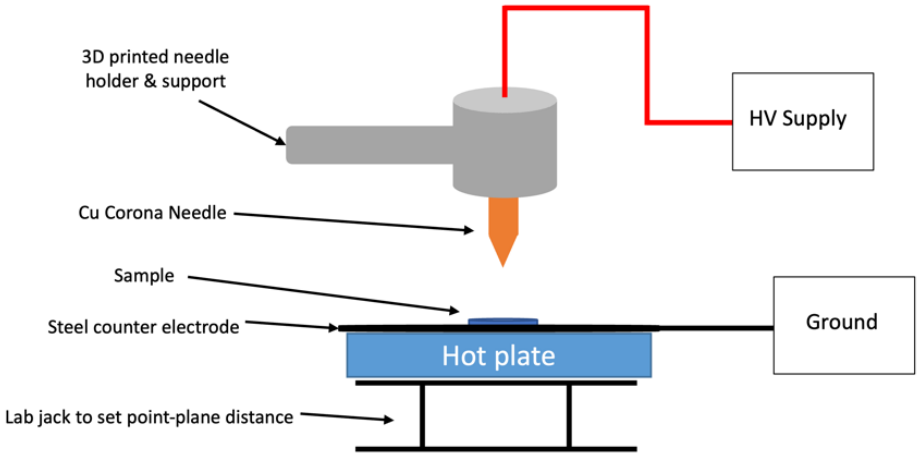

Figure S4. Schematic of corona discharge poling station.

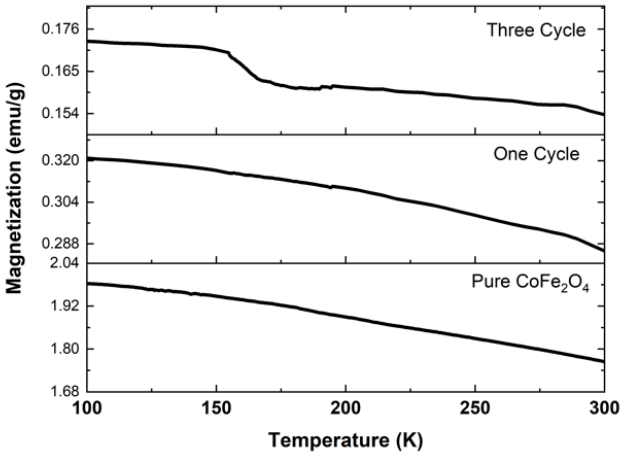

Figure S5. SQUID magnetization vs temperature sweeps (field-cooled) from 300 to 100K for pure $CoFe_2O_4$ nanowires, core-shell nanowires from one wetting cycle, and three wetting cycles. A change in magnetization is observed near the orthorhombic to rhombohedral phase transition

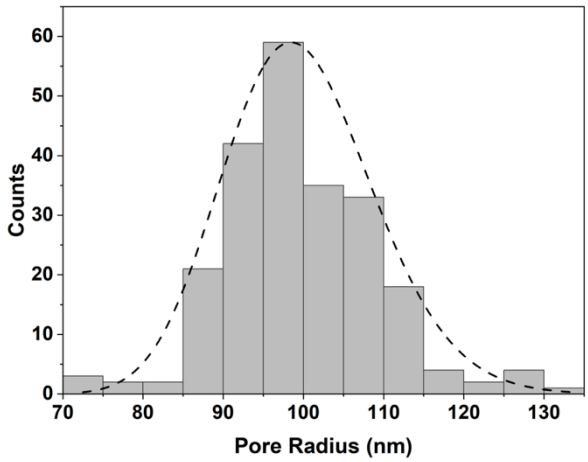

for $BaTiO_3$ near 170K is indirect evidence for magnetoelectric coupling in the nanowires.

Figure S6. Pore radius distribution of an empty AAO template prior to nanowire deposition.

References:

1 L. R. Prado, N. S. De Resende, R. S. Silva, S. M. S. Egues and G. R. Salazar-Banda, *Chemical Engineering and Processing: Process Intensification*, 2016, **103**, 12–20.
2 U. A. Joshi, S. Yoon, S. Baik and J. S. Lee, *J. Phys. Chem. B*, 2006, **110**, 12249–12256.
3 T.-C. Huang, M.-T. Wang, H.-S. Sheu and W.-F. Hsieh, *J. Phys.: Condens. Matter*, 2007, **19**, 476212.
4 F. Li, T. Wang, L. Ren and J. Sun, *J. Phys.: Condens. Matter*, 2004, **16**, 8053–8060.
5 K. Nielsch, J. Choi, K. Schwirn, R. B. Wehrspohn and U. Go, *Nano Lett.*